RESEARCH PAPER

Tandem Preparation of Furo[3,2-c]Coumarin Derivations Using Nano-Sized Fe_3O_4/N-GQDs Composite as a Magnetic Nanocatalyst

Sakineh Esfandiari Baghbamidi

Department of Chemistry, Bandar Abbas Branch, Islamic Azad University, Bandar Abbas, Iran

ARTICLE INFO

Article History:
Received 03 July 2024
Accepted 22 September 2024
Published 01 October 2024

Keywords:
Fe_3O_4 nanoparticles
Furo[3,2-c]coumarin
Graphene quantum dots
Tandem reactions

ABSTRACT

Nitrogen-doped graphene quantum dots (N-GQDs), which are less than 10 nm in size, are an interesting member of carbon nanomaterials. N-GQDs nanostructures have been broadly used in several fields such as drug-gene delivery systems, photocatalytic reactions, and catalysts owing to their unique properties. However, N-GQDs have rarely been introduced as a catalyst in organic synthesis. Herein, Fe_3O_4 nanoparticles are prepared via the co-precipitation method. Due to further active sites on the surface of nanocomposites, nano-sized Fe_3O_4/N-GQDs composite can affect the catalytic activities. Also, the new nano-sized Fe_3O_4/N-GQDs magnetic composite has been well prepared by a green, low-cost, and easy co-precipitation route. The developing concern for sustainability in the chemical industry has led to the growth of "green chemistry", which aims to limit the use of hazardous substances. One-pot multicomponent reactions (MCRs) are one of the powerful approaches to preparing a wide range of organic compounds. This protocol's advantages in organic compound preparation include atom economy, good to excellent yields (up to 90%), short reaction time (28 min), a wide range of various products, and high catalytic activities. In this research, furo[3,2-*c*]coumarin derivations were prepared via microwave conditions using Fe_3O_4/N-GQDs composite as a nanocatalyst.

How to cite this article
Esfandiari Baghbamidi S. Tandem Preparation of Furo[3,2-c]Coumarin Derivations Using Nano-Sized Fe_3O_4/N-GQDs Composite as a Magnetic Nanocatalyst. J Nanostruct, 2024; 14(4):1272-1279. DOI: 10.22052/JNS.2024.04.026

INTRODUCTION

Furo[3,2-*c*]coumarin scaffolds are one of the famous heterocyclic compounds due to their potential and wide spectrum of biological activities including anticancer [1], antibacterial [2], antifungal [3], immunotoxicity [4], anticholinesterase [5], and anti-HIV [6]. Therefore, these compounds are attractive targets in organic and medicinal chemistry. The preparation of bioactive heterocyclic compounds from available starting substances via one-pot multicomponent reactions (MCRs) has gained remarkable interest in both synthetic and medicinal chemists [7]. MCRs are extremely well suited for diversity-oriented synthesis and lead to the connection of three or more starting substances in a single process with high atom economy and bond-forming efficiency [8-10]. The possibility of accomplishing MCRs under mild conditions with a natural catalyst such as amino acids could improve their effectiveness from cost-effectiveness and ecological points of view [11].Several methods have been reported

* *Corresponding Author Email: esfandiari.576@yahoo.com*

for the preparation of the *trans*-furo[3,2-*c*] coumarin scaffolds using diverse catalysts, for instance, pyridine or a mixture of acetic acid/ ammonium acetate [12], ionic liquid [BMIm]OH [13], palladium(II) trifluoroacetate [14], copper(II) bromide [15], N-methylimidazolium [16], and triethylamine [17]. Some of these synthesis methods have specific disadvantages: long reaction times, using toxic materials, and specific conditions.

In recent decades, several categories of carbon nanomaterials such as graphene quantum dots (GQDs) have been developed due to their exceptional physicochemical attributes [18]. GQDs reveal many interesting attributes. These attributes have their origins in their distinguished structure features [19]. Moreover, the presence of functional groups (*e.g.* hydroxyl and carboxyl) on the edge of GQDs structures can be used as bonding agents to the substrate or coating materials. On the other hand, some reports indicated that heteroatom doping of GQDs such as nitrogen, sulfur, and phosphorus can successfully increase more active sites owing to the modulated bandgap [20-22]. Also, retrieving these carbon nanostructures from the reaction environment could be modified with diverse materials such as nanomaterials, organic compounds, polymers, *etc*. [23]. Among them, magnetic nanostructures are of sharp interest to investigators due to their outstanding magnetic attributes [24]. Moreover, structural comparative studies indicate that magnetically attributes of metal oxide nanocomposites were superior to bulk form [25, 26]. N- GQDs/Fe_3O_4 nanocomposite is one of the most practical soft-magnetic compounds due to its low price, nontoxicity, chemical stability, and high resistance to erosion [27-29].

Herein we reported the use of Fe_3O_4/N-GQDs nanocomposites as a catalyst for the preparation of furo[3,2-*c*]coumarin derivatives using a multicomponent reaction of 2,4′-dibromoacetophenone, various benzaldehydes, and 4-hydroxycoumarin under microwave irradiation conditions in ethanol.

MATERIALS AND METHODS

Materials

The chemicals were purchased straight from ACROS Company in high purity. All of the chemicals were applied without further purification. The as-prepared products were characterized by melting point, FT-IR, and $^{1}H/^{13}C$ NMR. All melting points were measured in capillary tubes on a Boetius melting point microscope. Also, an investigation of FT-IR was recorded on a WQF-

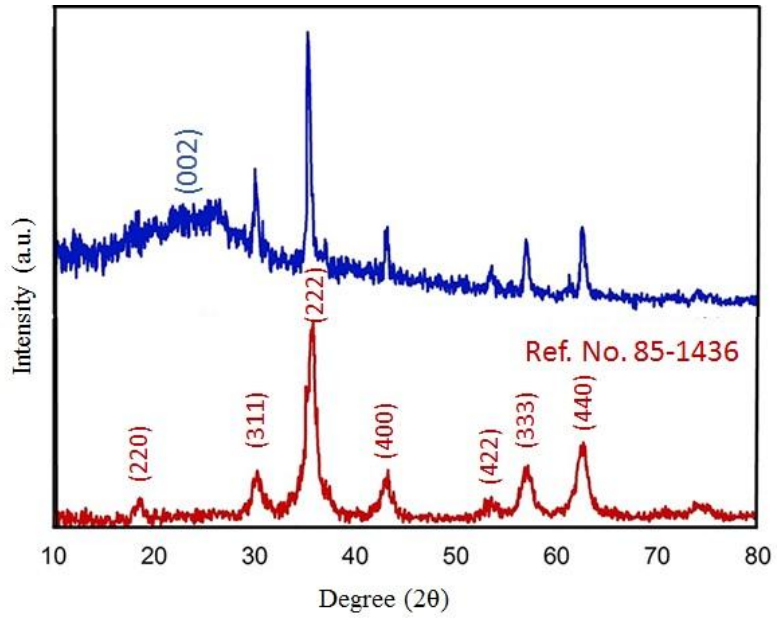

Fig. 1. XRD patterns of pure Fe_3O_4 nanoparticles (up) and Fe_3O_4/N-GQDs nanocomposite (down).

510 spectrometer 550 Nicolet. In addition, $^{1}H/^{13}C$ NMR was investigated on Bruker Avance-400 MHz spectrometers in the presence of chloroform-*d* as solvents (TMS is an internal standard).

Preparation of Fe_3O_4 nanoparticles

1.4 g of $FeSO_4.7H_2O$ and 2 g of $Fe_2(SO_4)_3$ were dissolved in 100 ml of double-distilled water. The concentrated ammonium hydroxide solution (25%) was added dropwise to adjust the pH= 10. The mixture was continually stirred at 60 °C for 1 hour at room temperature. The solid nanoparticles were collected by an external magnet, washed with distilled water (4×20 ml), and then dried at 40 °C for 4 hours under vacuum.

Preparation of Fe_3O_4@N-GQDs nanoparticles

The mixture of 1 g of citric acid, 0.4 ml of ethylenediamine, and 50 ml of double-distilled water was stirred for 2 minutes at room temperature to form a clear homogeneous mixture. Then, the 1 g of as-prepared Fe_3O_4 magnetic nanocomposite was poured into the above mixture and sonicated for 1 min to make a homogeneous mixture. Afterward, the mixture was put in a 150 ml Teflon Lined stainless steel autoclave and placed in the electric oven at 180 °C for 9 hours under hydrothermal conditions. At completion, the magnetic solid was collected by external magnetic and washed with dry ethanol (4×20 ml). The separated solid, finally, dried at 60 °C for 24 hours under vacuum conditions.

Preparation of furo[3,2-c]coumarin derivatives using Fe_3O_4@N-GQDs nanoparticles as a catalyst

An equivalent mixture of 2,4′-dibromoacetophenone and pyridine was stirred (1 min). After that, 4-hydroxycoumarin (1 mmol), various benzaldehyde (1 mmol), Fe_3O_4@N-GQDs nanoparticles (0.30 g), and ethanol (10 ml) was added to the above mixture. The mixture was stirred. Next, the reaction was continuted under microwave conditions. The reaction progress was checked out by thin-layer chromatography (TLC). After completion, the crude products were washed with ethanol. To give a pure product, the recrystallization from ethanol was done.

RESULTS AND DISCUSSION

The XRD graphs of pure magnetic Fe_3O_4 and

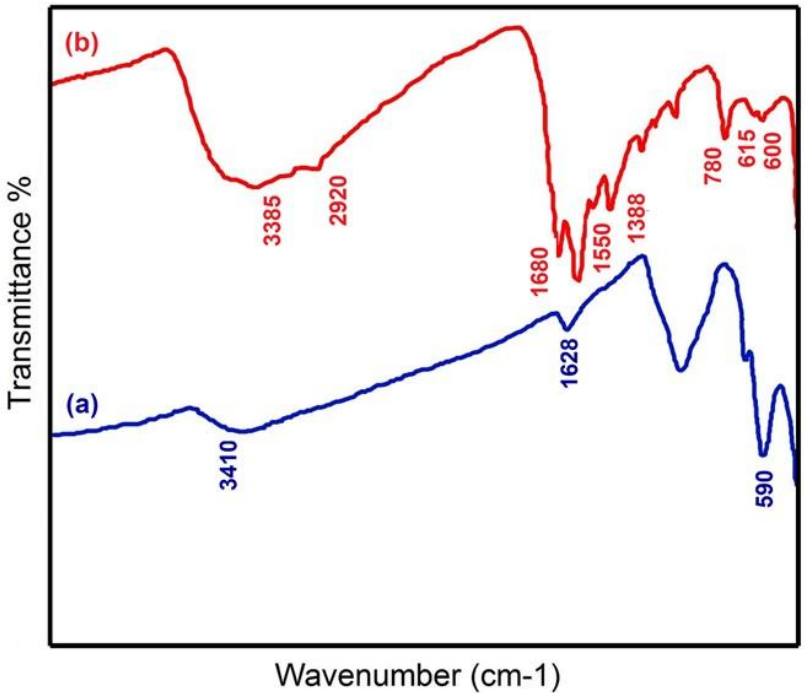

Fig. 2. FT-IR spectrum of pure Fe_3O_4 nanoparticles (a) and Fe_3O_4/N-GQDs nanocomposite (b).

Fe_3O4/N-GQDs nanocomposite were indicated in Fig. 1. As presented in Fig. 1a, diffraction angles (2ϑ) for magnetic nanoparticles evident at ~ 35.7°, 38°, 43.4°, 53.8°, 57.3°, and 62.9° can be indexed to (220), (311), (222), (400), (422), (511), and (440) plans, according to Fe_3O_4 cubic spinel structure (JCPDS Card No. 85-1436). In the case of the final graph, a broad peak at 2ϑ= 24° (002 plane) can be related to the amorphous structure of N-GQDs. According to the final graph, all Bragg peaks of nano-sized Fe_3O_4 particles and N-GQDs are seen at the same time and the Fe_3O_4/N-GQDs phase compositions did not change.

The surface functional groups of pure Fe_3O_4 magnetic and Fe_3O_4/N-GQDs nanocomposites were confirmed by FT-IR spectroscopy (Fig. 2). Absorption peak at 590 cm^{-1} is related to Fe-O. Also, absorbance peaks at 1628 cm^{-1} and 3410 cm^{-1} related to OH bending and stretching vibration, respectively, due to absorbed H_2O by the surface of nanoparticles (Fig. 2a). As compared with pure Fe_3O_4 spectra, the new bands at 1680 cm^{-1}, 1550 cm^{-1}, and 1388 cm^{-1} were corresponded to stretching vibration peaks of C=O, C=C, and C-O/C-N, respectively. In addition, a peak located at 3385 cm^{-1} is related to the vibration of -OH stretching. Also, absorbance peaks approximately at 3198 cm^{-1} and 2920 cm^{-1} were related to $=CH_{sp2}$

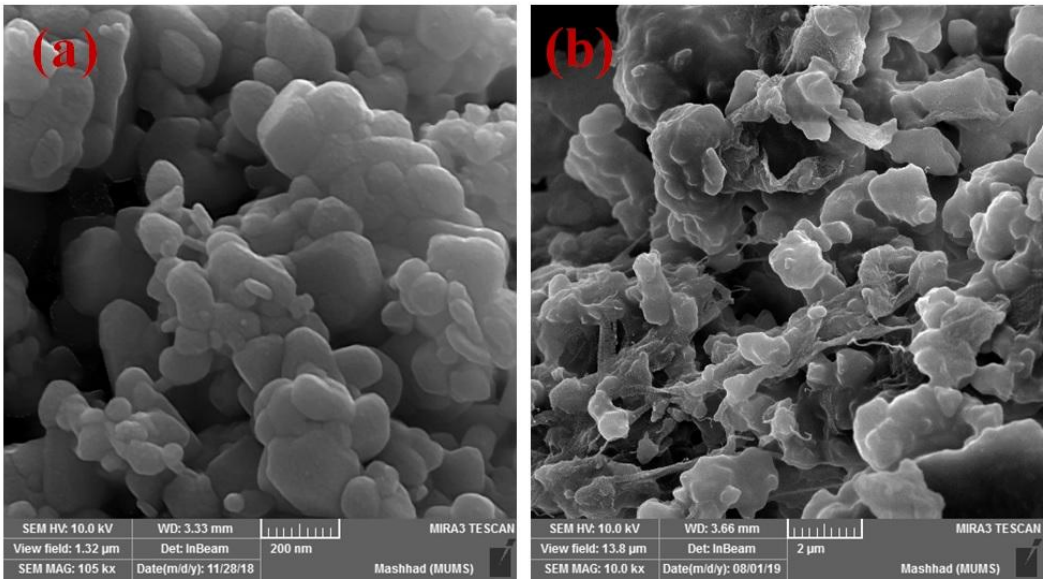

Fig. 3. FE-SEM images of pure Fe_3O_4 nanoparticles (a) and Fe_3O_4/N-GQDs nanocomposite (b).

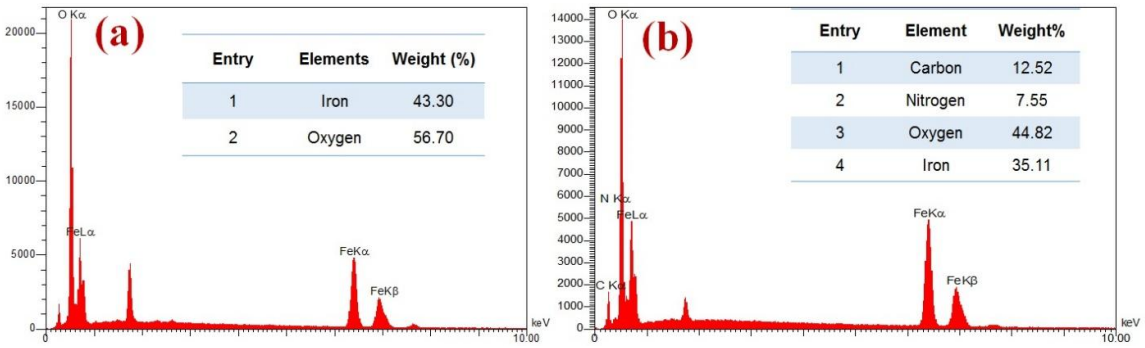

Fig. 4. EDX analysis results of the pure Fe_3O_4 nanoparticles (a) and Fe_3O_4/N-GQDs nanocomposite (b).

and -CH_{sp3} (Fig. 2b).

The investigation of surface morphology and particle size was done by the FE-SEM method. Moreover, the purity of Fe_3O_4 and Fe_3O_4/N-GQDs nanocomposites was studied by EDX analysis. The results of the investigation of morphology and element distribution were revealed in Fig. 3 and Fig. 4, respectively. Fig. 3a reveals the formation of Fe_3O_4 nanoparticles. According to the Fig. 3b, N-GQDs completely cover the surface of the Fe_3O_4 nanoparticles. From Fig. 4a, results show that as-prepared nanoparticles contain just two elements: Fe (43.30 %) and O (56.70 %). Besides, the final EDX data confirm not only the presence of the Fe_3O_4 nanoparticles but also the formation of the carbon (12.52) and nitrogen (7.55) in the final nanostructure (Fe_3O_4/N-GQDs nanocomposites).

To determine the optimal conditions for the preparation of the furo[3,2-c]coumarin derivatives, we developed the effect of temperature, solvent, and catalyst amount on the model reaction of 2,4′-dibromoacetophenone (1 mmol), benzaldehyde (1 mmol), and 4-hydroxycoumarin (1 mmol). The model reactions were done using

Table 1. Optimization of the model reaction in the presence of various catalysts [a].

No.	Catalyst	Solvent	Time (min)	Yield (%)[b]	Ref.
1	Acetic acid (20 mol%)	EtOH	55	15	[15]
2	Acetic acid (20 mol%)	CH_3CN	70	10	[15]
3	Tosylic acid (0.35 g)	EtOH	55	33	[14]
4	Tosylic acid (0.35 g)	CH_3CN	60	38	[14]
5	Pipyridine (20 mol%)	CH_3CN	45	50	[6]
6	Pipyridine (20 mol%)	EtOH	40	58	[6]
7	Et_3N (15 mol%)	CH_3CN	35	61	[2]
8	Et_3N (15 mol%)	EtOH	35	68	[2]
9	Fe_3O_4/N-GQDs (0.30 g)	H_2O	28	63	This Job
10	Fe_3O_4/N-GQDs (0.30 g)	CH_3CN	28	71	This Job
11	Fe_3O_4/N-GQDs (0.30 g)	DMF	28	58	This Job
12	Fe_3O_4/N-GQDs (0.20 g)	EtOH	35	80	This Job
13	Fe_3O_4/N-GQDs (0.30 g)	EtOH	28	90	This Job
14	Fe_3O_4/N-GQDs (0.40 g)	EtOH	25	90	This Job

[a] 4-hydroxycoumarin (1 mmol), 2,4′-Dibromoacetophenone (1 mmol), benzaldehyde (1 mmol).
[b] Isolated yield.

Table 2. Microwave-assisted preparation of furo[3,2-*c*]coumarin derivatives in the presence of Fe_3O_4/N-GQDs (0.30 g) in ethanol.

No.	Aldehyde (R)	Product	Time (min)	Yield (%)[a]	M.p. (ºC)
1	H	4a	30	93	243-244
2	3-Me	4b	35	87	222-224
3	2-Me	4c	40	85	171-173
4	2-Cl	4d	30	93	219-221
5	4-Cl	4e	30	95	250-252
6	2-NO_2	4f	30	92	232-234
7	4-SCH_3	4g	35	87	206-208
8	4-Br	4h	30	94	256-258
9	3-NO_2	4i	30	92	250-252
10	4-Me	4j	35	88	204-206
11	2-F	4k	30	92	186-188

[a] Isolated yield.

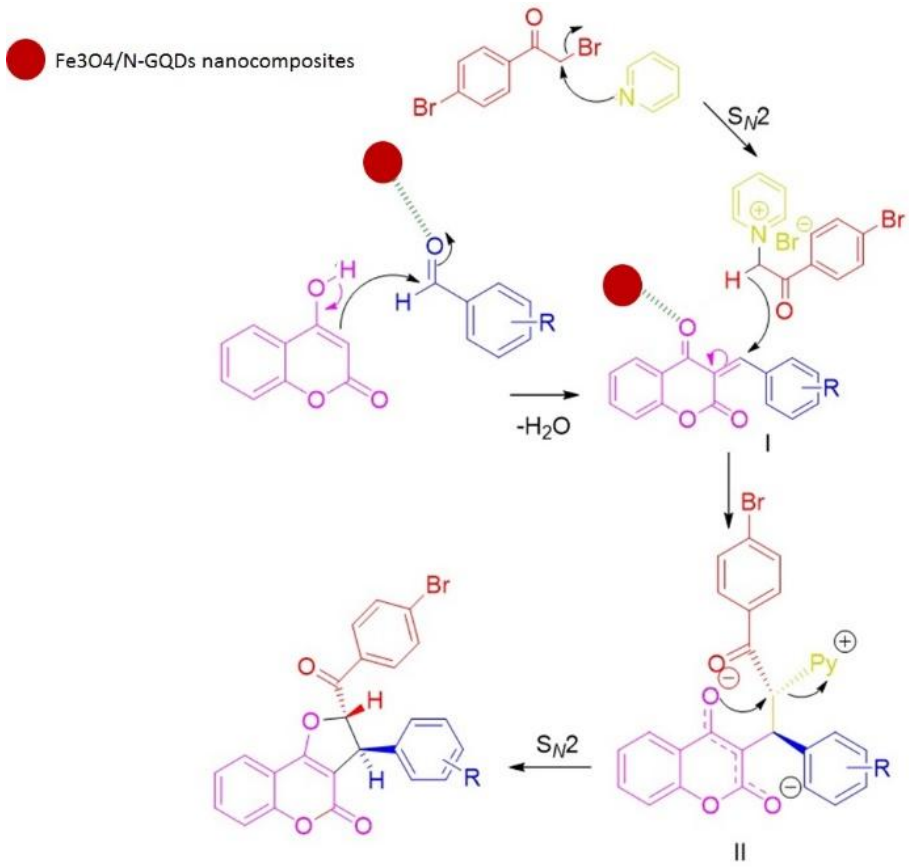

Fig. 5. The proposed mechanism.

various catalysts: acetic acid, tosylic acid, piperidine, and triethylamine. When the reaction was done in the presence of Fe_3O_4/N-GQDs nanocomposite (0.30 g) as the nanocatalyst, the product could be obtained in good yield. Some reactions were investigated in the presence of various solvents such as water, acetonitrile, dimethylformamide, and ethanol. The best data were observed under microwave conditions in ethanol. It was found that the reaction gave satisfying data in the presence of nanocom Fe_3O_4/N-GQDs nanocomposite (0.30 g) which gave excellent yields of products (Table 1). With these hopeful data in hand, we turned to study the scope of the reaction using various benzaldehydes as substrates under the optimized reaction conditions (Table 2). It was revealed that aromatic aldehydes with electron-withdrawing groups reacted faster than those with electron-releasing groups. Meanwhile, it has been observed that better yields are obtained with substrates having electron-withdrawing groups.

Fig. 5 revealed the reasonable mechanism for the preparation of furo[3,2-*c*]coumarin derivatives in the presence of Fe_3O_4/N-GQDs nanocomposite. Based on our studies of mechanism, the reaction starts with a *K*noevenagel condensation between benzaldehyde and 4-hydroxycoumarin to form the intermediate (I) on the active sites of Fe_3O_4/N-GQDs nanocomposite, which are chiefly responsible for the catalytic activity. Then, the Michael addition of pyridinium ylide with enones affords a zwitterionic intermediate and followed by cyclization affords the titled product. The final step is a S_N2 substitution reaction. The stereochemistry of the S_N2 reaction required a nucleophilic enolate attack from the back side of the electrophilic carbon atom bearing the leaving pyridinium group. Thus, the furo[3,2-*c*]coumarin is formed as the only product [17].

CONCLUSION

We provide a straightforward and

environmentally friendly protocol for the preparation of the furo[3,2-*c*]coumarin derivations catalyzed by Fe_3O_4/N-GQDs nanocomposite as a magnetic catalyst. The remarkable catalytic activity was greatly related to uniformity and available active sites on the surface of the catalyst. Then, Fe_3O_4 nanoparticles were decorated with N-GQDs. It is found that the joining of N-GQDs and Fe_3O_4 has a remarkable impact on catalytic activity improvement. Therefore, the tandem multicomponent reactions protocol has some benefits, for instance, good yield reaction (up to 90%), low reaction times (20 min), and low-cost and available catalysts. Moreover, using mild conditions led to an increased reaction rate and saved energy. In addition, the present approach can be used for the design of libraries and diversity-oriented synthesis and has potential for biological applications and drug discovery.

CONFLICT OF INTEREST

The authors declare that there is no conflict of interests regarding the publication of this manuscript.

REFERENCES

1. Wang X, Bastow KF, Sun C-M, Lin Y-L, Yu H-J, Don M-J, et al. Antitumor Agents. 239. Isolation, Structure Elucidation, Total Synthesis, and Anti-Breast Cancer Activity of Neo-tanshinlactone from Salvia miltiorrhiza. J Med Chem. 2004;47(23):5816-5819.
2. Safaei-Ghomi J, Babaei P, Shahbazi-Alavi H, Zahedi S. Diastereoselective synthesis of trans -2,3-dihydrofuro[3,2-c] coumarins by MgO nanoparticles under ultrasonic irradiation. Journal of Saudi Chemical Society. 2017;21(8):929-937.
3. Marzano C, Chilin A, Baccichetti F, Bettio F, Guiotto A, Miolo G, et al. 1,4,8-Trimethylfuro[2,3-H]quinolin-2(1H)-one, a new furocoumarin bioisoster. Eur J Med Chem. 2004;39(5):411-419.
4. Piccagli L, Borgatti M, Nicolis E, Bianchi N, Mancini I, Lampronti I, et al. Virtual screening against nuclear factor κB (NF-κB) of a focus library: Identification of bioactive furocoumarin derivatives inhibiting NF-κB dependent biological functions involved in cystic fibrosis. Bioorganic & Medicinal Chemistry. 2010;18(23):8341-8349.
5. Patel NB, Khan IH, Pannecouque C, De Clercq E. Anti-HIV, antimycobacterial and antimicrobial studies of newly synthesized 1,2,4-triazole clubbed benzothiazoles. Med Chem Res. 2012;22(3):1320-1329.
6. Al-Sehemi AG, El-Gogary SR. Synthesis and Photooxygenation of Furo[3,2-c]coumarin Derivatives as Antibacterial and DNA Intercalating Agent. Chin J Chem. 2012;30(2):316-320.
7. Babaei P, Safaei-Ghomi J, Rashki S, Mahmoudi Kharazm A. Morphology modified by polyvinylpyrrolidone for enhanced antibacterial and catalytic execution of bioactive Ag/ZnO composites based on hydroxyapatite in the synthesis of O-Aminocarbonitriles. Ceram Int. 2023;49(14):22826-22836.
8. Abou-Shehada S, Mampuys P, Maes BUW, Clark JH, Summerton L. An evaluation of credentials of a multicomponent reaction for the synthesis of isothioureas through the use of a holistic CHEM21 green metrics toolkit. Green Chem. 2017;19(1):249-258.
9. Wang Z, Domling A. Multicomponent Reactions in Medicinal Chemistry. Multicomponent Reactions towards Heterocycles: Wiley; 2021. p. 91-137.
10. Zarganes-Tzitzikas T, Dömling A. Modern Multicomponent Reactions for better Drug Syntheses**. Organic chemistry frontiers : an international journal of organic chemistry. 2014;1(7):834-837.
11. Babaei P, Safaei-Ghomi J. Engineered N-doped graphene quantum dots/$CoFe_2O_4$ spherical composites as a robust and retrievable catalyst: fabrication, characterization, and catalytic performance investigation in microwave-assisted synthesis of quinoline-3-carbonitrile derivatives. RSC advances. 2021;11(55):34724-34734.
12. Altieri E, Cordaro M, Grassi G, Risitano F, Scala A. Regio and diastereoselective synthesis of functionalized 2,3-dihydrofuro[3,2-c]coumarins via a one-pot three-component reaction. Tetrahedron. 2010;66(49):9493-9496.
13. Rajesh SM, Perumal S, Menéndez JC, Pandian S, Murugesan R. Facile ionic liquid-mediated, three-component sequential reactions for the green, regio- and diastereoselective synthesis of furocoumarins. Tetrahedron. 2012;68(27-28):5631-5636.
14. Tan X-c, Zhao H-y, Pan Y-m, Wu N, Wang H-s, Chen Z-f. Atom-economical chemoselective synthesis of furocoumarins via cascade palladium catalyzed oxidative alkoxylation of 4-oxohydrocoumarins and alkenes. RSC Advances. 2015;5(7):4972-4975.
15. Zhang WL, Yue SN, Shen YM, Hu HY, Meng QH, Wu H, et al. Copper(ii) bromide-catalyzed intramolecular decarboxylative functionalization to form a C(sp3)–O bond for the synthesis of furo[3,2-c]coumarins. Organic & Biomolecular Chemistry. 2015;13(12):3602-3609.
16. Kumar A, Srivastava S, Gupta G. Cascade [4 + 1] annulation via more environmentally friendly nitrogen ylides in water: synthesis of bicyclic and tricyclic fused dihydrofurans. Green Chem. 2012;14(12):3269.
17. Wang Q-F, Hou H, Hui L, Yan C-G. Diastereoselective Synthesis of trans-2,3-Dihydrofurans with Pyridinium Ylide Assisted Tandem Reaction. The Journal of Organic Chemistry. 2009;74(19):7403-7406.
18. Yan T, Zhang X, Ren X, Lu Y, Li J, Sun M, et al. Fabrication of N-GQDs and AgBiS2 dual-sensitized ZIFs-derived hollow $Zn_xCo_{3x}O_4$ dodecahedron for sensitive photoelectrochemical aptasensing of ampicillin. Sensors Actuators B: Chem. 2020;320:128387.
19. Xi F, Zhao J, Shen C, He J, Chen J, Yan Y, et al. Amphiphilic graphene quantum dots as a new class of surfactants. Carbon. 2019;153:127-135.
20. Zhao H, Chang Y, Liu M, Gao S, Yu H, Quan X. A universal immunosensing strategy based on regulation of the interaction between graphene and graphene quantum dots. Chem Commun. 2013;49(3):234-236.
21. Jiang BK, Chen AY, Gu JF, Fan JT, Liu Y, Wang P, et al. Corrosion resistance enhancement of magnesium alloy by N-doped graphene quantum dots and polymethyltrimethoxysilane composite coating. Carbon. 2020;157:537-548.
22. Limchoowong N, Sricharoen P, Areerob Y, Nuengmatcha P, Sripakdee T, Techawongstien S, et al. Preconcentration and trace determination of copper (II) in Thai food recipes using

Fe_3O_4@Chi–GQDs nanocomposites as a new magnetic adsorbent. Food Chem. 2017;230:388-397.
23. Gholinejad M, Ahmadi J, Nájera C, Seyedhamzeh M, Zareh F, Kompany-Zareh M. Graphene Quantum Dot Modified Fe_3O_4 Nanoparticles Stabilize PdCu Nanoparticles for Enhanced Catalytic Activity in the Sonogashira Reaction. ChemCatChem. 2017;9(8):1442-1449.
24. Jesus ACB, Jesus JR, Lima RJS, Moura KO, Almeida JMA, Duque JGS, et al. Synthesis and magnetic interaction on concentrated Fe3O4 nanoparticles obtained by the co-precipitation and hydrothermal chemical methods. Ceram Int. 2020;46(8):11149-11153.
25. Yang J-S, Pai DZ, Chiang W-H. Microplasma-enhanced synthesis of colloidal graphene quantum dots at ambient conditions. Carbon. 2019;153:315-319.
26. Deng S, Fu A, Junaid M, Wang Y, Yin Q, Fu C, et al. Nitrogen-doped graphene quantum dots (N-GQDs) perturb redox-sensitive system via the selective inhibition of antioxidant enzyme activities in zebrafish. Biomaterials. 2019;206:61-72.
27. Wang Q, Yang Z. Industrial water pollution, water environment treatment, and health risks in China. Environ Pollut. 2016;218:358-365.
28. Shao S, Chen X, Chen Y, Zhang L, Kim HW, Kim SS. ZnO Nanosheets Modified with Graphene Quantum Dots and SnO_2 Quantum Nanoparticles for Room-Temperature H_2S Sensing. ACS Applied Nano Materials. 2020;3(6):5220-5230.
29. Naghshbandi Z, Arsalani N, Zakerhamidi MS, Geckeler KE. A novel synthesis of magnetic and photoluminescent graphene quantum dots/MFe2O4 (M = Ni, Co) nanocomposites for catalytic application. Appl Surf Sci. 2018;443:484-491.